MATERIALS CHEMISTRY FRONTIERS

RESEARCH ARTICLE

View Article Online
View Journal | View Issue

Cite this: *Mater. Chem. Front.*, 2025, **9**, 2943

Surface and grain boundary passivation using tetraphenylethylene derivative for high-performance perovskite solar cell

Shubhangi Bhardwaj, [a] Praveen Naik, [b] Anuj Kumar Palariya, [b] Smrutiranjan Panda, [a] Satish Patil *[b] and Sushobhan Avasthi *[a]

The efficiency of perovskite solar cells is constrained by surface and bulk recombination, along with poor band alignment at the interfaces of the transport layers. In our study, we demonstrate that modifying the surface and grain boundary (GB) of perovskite using tetraphenylethylene-enamine (TPE-en) enhances band alignment at the perovskite-hole transport layer interface and mitigates recombination within the perovskite material. By leveraging the solubility of small organic molecules in orthogonal solvents, we introduce TPE-en onto the perovskite surface akin to anti-solvent methods. Our investigation reveals a significant enhancement in the short circuit current density, fill factor, and open circuit voltage of the surface-modified (SM) perovskite. Specifically, we achieve a total power conversion efficiency of 18.73% ($MA_{0.9}AA_{0.1}PbI_3$). Comparative analyses show TPE-en outperforms other reported TPE derivatives in device performance. Through systematic interface analysis, we observe that TPE-en effectively reduces surface and GB defects by elevating the HOMO levels of the perovskite, introducing an interface dipole at the perovskite-spiro-OMeTAD interface. Optical measurements such as time-resolved photoluminescence, Ultraviolet photoelectron spectroscopy, and X-ray photoelectron spectroscopy were used to investigate the cause of this improvement. A 0.28 eV surface dipole formed provided effective band alignment, resulting in enhanced hole extraction and photovoltaic performance.

Received 20th March 2025,
Accepted 15th August 2025

DOI: 10.1039/d5qm00255a

rsc.li/frontiers-materials

1. Introduction

The hybrid organic–inorganic perovskite solar cell is a leading contender in emerging low-cost photovoltaic technologies.[1–6] State-of-the-art perovskite solar cells (PSCs) feature a perovskite layer sandwiched between electron and hole-transporting layers (ETL and HTL).[7,8] However, the performance of these cells is constrained due to surface and bulk recombination, alongside band misalignment at these crucial interfaces.[9] The prevailing HTL, lithium bis(trifluoromethane sulfonyl)imide (LiTFSI) doped Spiro-OMeTAD, often falls short in optimizing efficiency and stability as it interacts with light and temperature.[10–14] Hence, restructuring interface engineering processes becomes imperative to tackle these challenges reliably and efficiently.

The entrapment of charge carriers at the surface of perovskite, arising from 2-D defects induced by lead and iodine dangling bonds, as well as defects at grain boundaries, poses a significant hindrance to efficient charge collection and aggravates recombination.[15–17] Traditional approaches to address these challenges involve chemical or field-effect passivation to regulate the electrical activity of surface defects. Several strategies have been explored, ranging from fine-tuning the perovskite composition to engineering solvents with additives and anti-solvents, alongside post-deposition annealing and incorporating thin interlayers and novel transport materials.[18–20] Among them, incorporating organic π-conjugated semiconducting materials coupled with Lewis's base units represents a noteworthy approach.[21] They serve a dual purpose, effectively combining trap-passivation and charge extraction functionalities, enhancing both photovoltage and photocurrent.[22–24] The Lewis base components efficiently passivate the Lewis acid traps, such as under-coordinated Pb ions and Pb clusters, present on the surface and at the grain boundaries of perovskite.[25,26]

In this context, we introduce the TPE-en, a tetraphenylethylene derivative of incorporating an enamine moiety, as a potent passivating agent for enhancing the surface properties of perovskite films. TPE-en is constructed with a tetraphenyl ethylene (TPE) backbone, a renowned component widely employed in organic electronics applications.[27,28] Its synthesis is based on readily available starting materials *via* straightforward condensation reactions that are amenable to gram-scale

[a] *Centre for Nanoscience and Engineering, Indian Institute of Science Bangalore, Bengaluru, Karnataka, 560012, India. E-mail: savasthi@iisc.ac.in*
[b] *Solid State and Structural Chemistry Unit, Indian Institute of Science Bangalore, Bengaluru, Karnataka, 560012, India. E-mail: spatil@iisc.ac.in*

production under mild conditions without any byproducts. While organic semiconductors often face scrutiny for stability and environmental impact, TPE-en's robust π-conjugated core may contribute to improved durability. Looking ahead, efforts should be directed toward greener synthetic approaches, life-cycle assessment, and evaluating economic feasibility to ensure scalability and sustainable commercialization.

TPE-en functions as the pivotal anchoring Lewis base, capable of passivating surface defects in the perovskite structure. Specifically, the enamine functional group embedded within TPE-en serves as the essential Lewis base.[29,30] The inherent properties of TPE core as Lewis base to interact with uncoordinated bonds of perovskite facilitates us to use it into perovskite surface *via*. Loading molecule with orthogonal solvent such as chlorobenzene (CB). Such advantageous features contribute to enhancing the efficiency of TPE-en in passivating surface defects and optimizing the dynamics of charge carriers in perovskite solar cells. Our research indicates that TPE-en can contribute to chemical passivation, field effect passivation, or both, while aligning energy levels. The decrease in defects was validated through progressively enhanced optoelectronic and device measurements.

2. Results and discussion

In this study, we present the utilization of an enamine-based organic material, TPE-en, as an effective passivation agent. TPE-en meets the essential criteria for an ideal passivation material, including solubility in various orthogonal solvents to perovskite, facilitating solution processability. Additionally, it possesses a substantial bandgap of 2.8 eV, with minimal absorption observed within the crucial range of 600–800 nm. Remarkably, solar cells employing TPE-en-modified double-cation perovskite exhibit a notable increase in power conversion efficiency (PCE) from 15.42% to 18.73% compared to pristine cells. Comparative analysis indicates superior performance of TPE-en over other reported TPE derivatives in terms of efficiency enhancement.

To elucidate the underlying mechanisms leading to enhanced efficiency, we conducted optical and electrical measurements. Our findings suggest that the introduction of TPE-en derivative induces interface dipoles at the perovskite surface, thereby enhancing band alignment at the perovskite-hole transport layer (HTL) interface. The novel enamine-based TPE derivative synthesized in this study is illustrated in Fig. 1a. Further investigation of the photo-physical properties of TPE-en through ultraviolet-visible (UV-Vis) absorption and steady-state photoluminescence (ss-PL) spectroscopy reveals predominant absorption of lower wavelengths (<450 nm). The band below 300 nm is associated with the π–π* transition of the π-conjugated backbone, while the band within the range of 300–450 nm is attributed to intramolecular charge transfer (ICT) between the periphery moieties and the core tetraphenylethylene group.

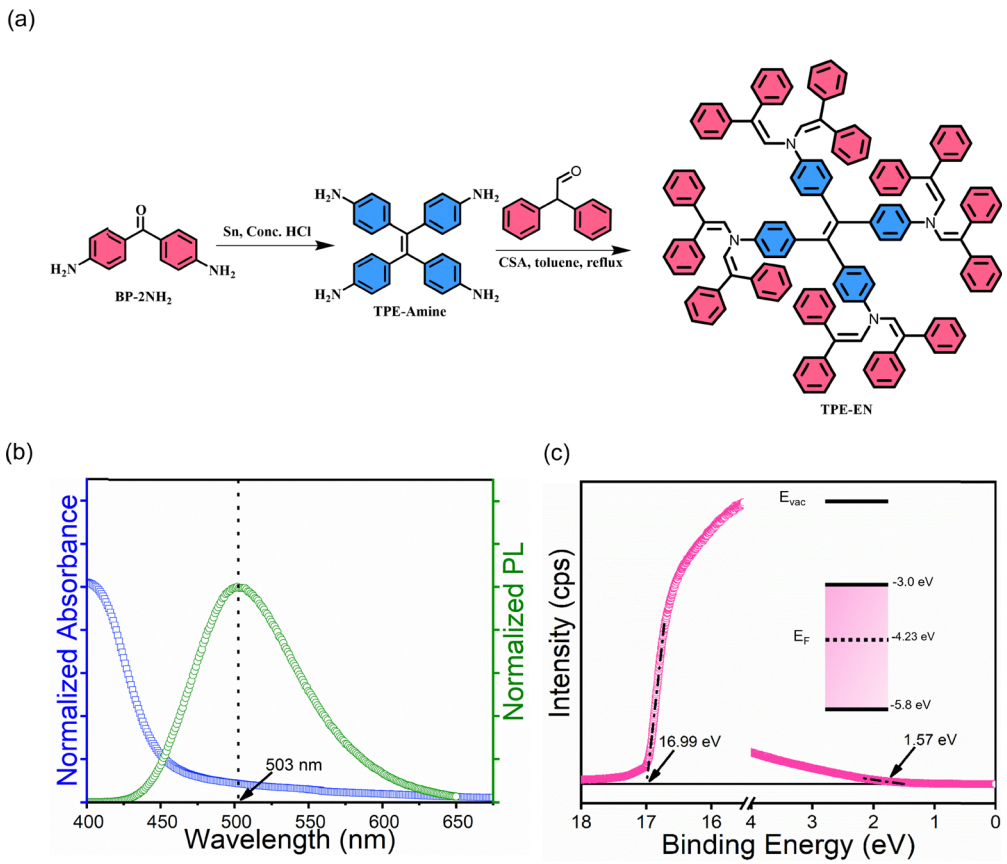

Fig. 1 (a) Synthetic pathway (b) Absorption and PL spectra and (c) UPS spectra of TPE-en.

A band gap of 2.8 eV is obtained by fitting the absorption edge using the Woods and Tauc equation (eqn (1) in SI).[31,32] For perovskite absorbers, our wavelength of interest is between 400–800 nm. The PL emission spectra ranges from 420 to 650 nm and is in conjunction with the absorption edge with an emission peak at 503 nm Fig. 1b. We are fabricating n–i–p devices with the perovskite/HTL interface on the far side of the light illumination. The photons reaching the perovskite/HTL interface have even longer wavelengths of 600–800 nm, for which TPE-en is effectively transparent, especially at thickness used here.

To understand the charge-transfer, we measured the HOMO and LUMO levels of TPE-en using ultraviolet photoelectron spectroscopy (UPS) (Fig. 1c). For a pristine TPE-en film the work function was −4.23 eV and HOMO level was −5.8 eV. Considering the material's band gap of 2.80 eV, we calculated the LUMO level as −3.0 eV. The films are also stable up to 413 °C (Fig. S1d).

One of the ways our work differs from previous attempts with other TPE derivatives is the way we incorporate the TPE-en in the perovskite layer. Here the TPE-en was included in the antisolvent (chlorobenzene) in the dilute concentration of 11.1% v/v (Fig. 2a). The method yields a quite a uniform distribution of TPE-en on perovskite (<5 nm at 11.1% v/v concentration) which is beyond the resolvable limit of a microscope (Fig. S4). From the histograms below (Fig. 2c–f) we observe the spread of device performance to be repeatable to a wide order, thus, despite its simplicity, the method of modifying perovskite surface is very consistent, showing that the TPE-en distribution is conformal and continuous.

Surface-modified (SM) perovskite devices show better device characteristics than pristine perovskite (from Fig. 2b). The photovoltaic parameters of the champion devices are listed in Table 1. The best pristine device yielded a short circuit current density of 21.27 mA cm^{-2}, open circuit voltage (V_{oc}) of 1.01 V, fill factor (FF) of 71.79%, and power conversion efficiency (PCE) of 15.43%.

In comparison, the photovoltaic data of SM perovskite is superior with champion device J_{sc} of 23.51 mA cm^{-2}, V_{oc} of 1.09 V, FF of 73.08%, and PCE of 18.73%. The enhancement is most noticeable in the short circuit current density (J_{sc}) and fill factor (FF), with a relative improvement of 8–13% and an absolute improvement of 2–8%, respectively.

The SM perovskite-based devices also show near-ideal diode behavior compared to pristine perovskite devices with ∼23% reduction in their ideality factor (n_{id}) (Table 1) and a reduction by an order in leakage current (J_o mA cm^{-2}). These results are all consistent with lower surface recombination, better band matching at the interface, and, consequently, longer carrier extraction length in the nip device.[33,34]

This improvement in the device due to the TPE-en could be attributed to chemical passivation or field-effect passivation, or both. The XRD pattern (Fig. S5) for the pristine and SM perovskite shows no shift in the material's peak position. Similarly, no change in the band gap is observed (Fig. 3a). Therefore, as expected, the unit cell structure of the perovskite films remains unaffected due to surface modification. However, the reduction in defects is readily seen in optical measurements. The gentle onset of optical absorption in the pristine perovskite is due to the defects at the band-edge (Fig. 3b). The disorder is quantified by Urbach energy which for pristine films is 89.2 meV, whereas the absorption onset is sharper for SM perovskite with an Urbach energy of 22.1 meV. Although optical

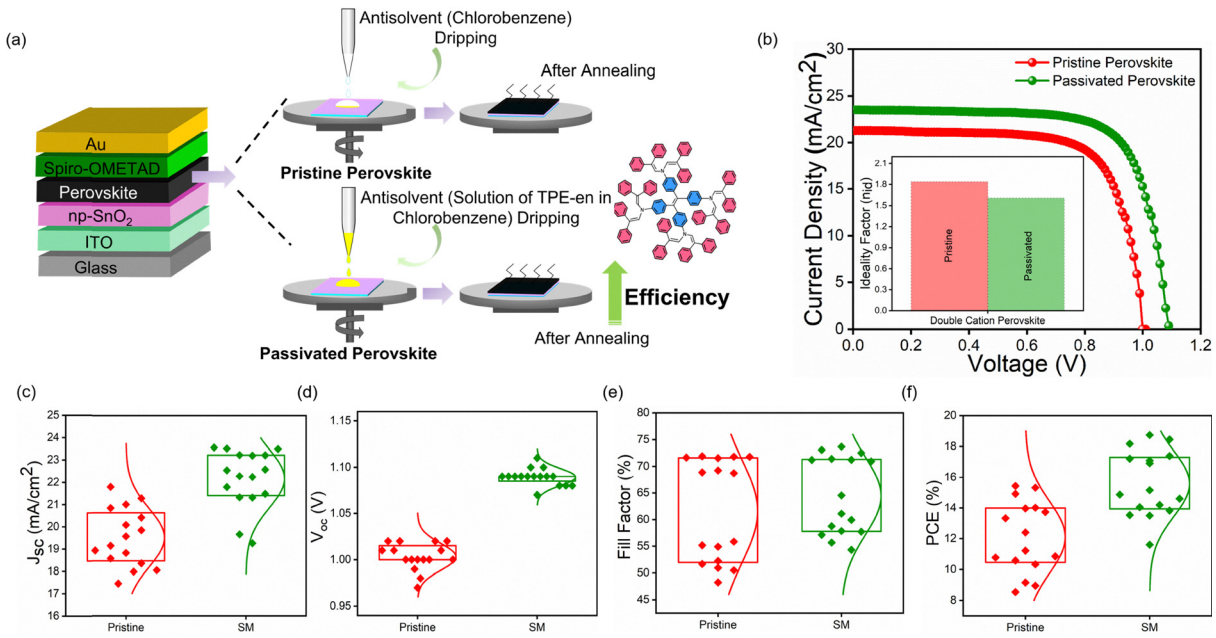

Fig. 2 (a) Device schematic and the deposition of pristine and SM perovskite, Light J–V characteristics and ideality factor of the champion cells using (b) Double cation perovskite $MA_{0.9}AA_{0.1}PbI_3$ (350 nm), (c)–(f) Statistics of current density (J_{sc}), open-circuit voltage (V_{oc}), fill factor (FF), and power conversion efficiency (PCE) for Pristine and SM perovskite with double cation perovskite as an absorber.

Table 1 Device parameters of the champion devices

Perovskite used	Variation	J_{sc} (mA cm^{-2})	V_{oc} (V)	FF (%)	η (%)	n_{id}	J_o ($\times$ 10^{-9} A cm^{-2})
$MA_{0.9}AA_{0.1}PbI_3$	Pristine	21.27	1.01	71.79	15.43	1.84	46
	SM	23.51	1.09	73.08	18.73	1.61	1.48

absorption is not the most accurate method to calculate Urbach tails,[35–37] however, the net reduction of 67.1 meV is significant. Due to the presence of TPE-en, there are fewer defects in SM perovskite than in pristine perovskite.

To confirm lower interface recombination, we also measure time resolved photoluminescence (TRPL). Noticeably, TRPL measurements were performed using picosecond laser diode of wavelength 673 nm as the excitation source to prevent any PL and lifetime contribution from the TPE-en which emits in the range of 420–650 nm. The transient PL signal was fit to a bi-exponential: $y = A_1 \times \exp(-x/\tau_1) + A_2 \times \exp(-x/\tau_2) + y_0$ (Fig. 3c). The faster decay component (τ_1) corresponds to the radiative recombination, and the slower decay component (τ_2) corresponds to the non-radiative recombination. A_1 and A_2 are the weight percentages associated with respective mechanisms. The calculated parameters are listed in Table 2. The τ_1 for pristine perovskite is 21.33 $\pm$ 1.67 ns, and for SM perovskite, it is 40.30 $\pm$ 1.44 ns and τ_2 for pristine perovskite is 813.57 $\pm$ 4.74 ns, and for SM perovskite, it is 1074.54 $\pm$ 118.21 ns. A slightly higher lifetime in SM perovskite implies a better charge carrier recombination lifetime.

The perovskite/transport-layer interface can be improved by (a) chemical passivation, (b) field-effect passivation or (c) better band alignment.[33] Dangling bonds at the perovskite surface are chemically eliminated in chemical passivation, reducing defects and carrier recombination. A surface electric field is established in field-effect passivation, which repels one type of carrier and limits carrier recombination.[38,39] Better band-alignment helps in efficient charge extraction, reducing carrier pile-up and recombination at the interface. While optical experiments confirm the lower recombination, they do not differentiate between these mechanisms. We use X-ray & Ultra-Violet Photoelectron Spectroscopy (XPS & UPS) to make the distinction. The XPS binding energy peaks for Pb $4f_{5/2}$ and Pb $4f_{7/2}$ in perovskites lie at 143.36 eV and 138.48 eV (Fig. 4a). These peaks don't shift after surface modification, implying the absence of any surface band-bending or electric-field.[40–43] The oxidation state of the Pb atoms is also unchanged, so chemical modification is ruled out.

UPS measurements were used to investigate the band-alignment. To the extent that XPS is sensitive, we do not see evidence of significant chemical or field-effect passivation. Fig. 4(b and c) shows the UPS curve for Pristine and SM perovskite and lithium-doped spiro-OMETAD. Fig. 4d shows the flat band diagram obtained from the UPS data. The introduction of TPE-en modifies the work function of the perovskite surface from -4.87 eV (pristine perovskite) to -4.59 eV (SM perovskite). The change in work function can be explained by the 0.2 eV surface dipole. TPE-en molecule has a dipole of 2.71 D (Fig. S2). Similar dipoles are seen in heterointerfaces of conjugated molecules,[44–46] which are known to change work-function.[42,46–48] The proposed dipolar/zwitterion state in the TPE-based twisted excited state system would get influenced by the extended conjugation that exists in the TPE-en based derivative.[49,50] The position of the HOMO level with respect to the vacuum level is -5.62 eV in SM perovskite, compared to -5.97 eV for pristine perovskite. The difference in the valence band edge of perovskite and HOMO of the spiro-OMeTAD gives the band-alignment at the interface. The relative shift of $\sim$0.35 eV, reduces the band-offset of the perovskite/spiro-OMeTAD interface by 70 meV, improving charge extraction. In summary, the device performance improves neither due to the chemical nor due to the field-effect passivation. Rather, a better band alignment at the perovskite/spiro-OMeTAD interface is responsible for the higher J_{SC} and FF in SM-perovskite.

We have compared the performance of TPE-en with other TPE-based derivatives such as TPE-4MDPA (*N*,*N*-di(4-methoxyphenyl)aminophenyl) with non-fused conjugated structure and TPE derivatives substituted with fused conjugated structure such as TPE-4cz (carbazole), and TPE-tcz (tertiary butyl carbazole) (Fig. S7).

These were synthesized as per the reported recipes.[51–57] Fig. 4e shows the light *JV* characteristics of the champion solar

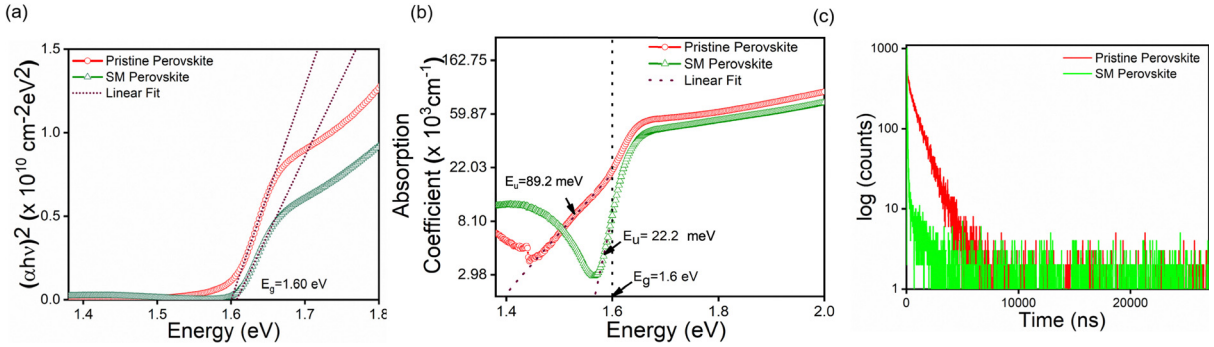

Fig. 3 (a) Tauc Plot, (b) absorption coefficient and (c) TRPL spectra of pristine and SM perovskite.

Table 2 Summary of lifetime parameters obtained from the bi-exponential fitting of PL decay curve

Variation	A_1 (%)	τ_1 (ns)	A_2 (%)	τ_2 (ns)	τ_{avg} (ns)
Pristine perovskite	3.55	21.33 ± 1.67	96.45	813.57 ± 4.74	812.8
SM perovskite	66.95	40.30 ± 1.44	33.05	1074.54 ± 118.21	1001.51

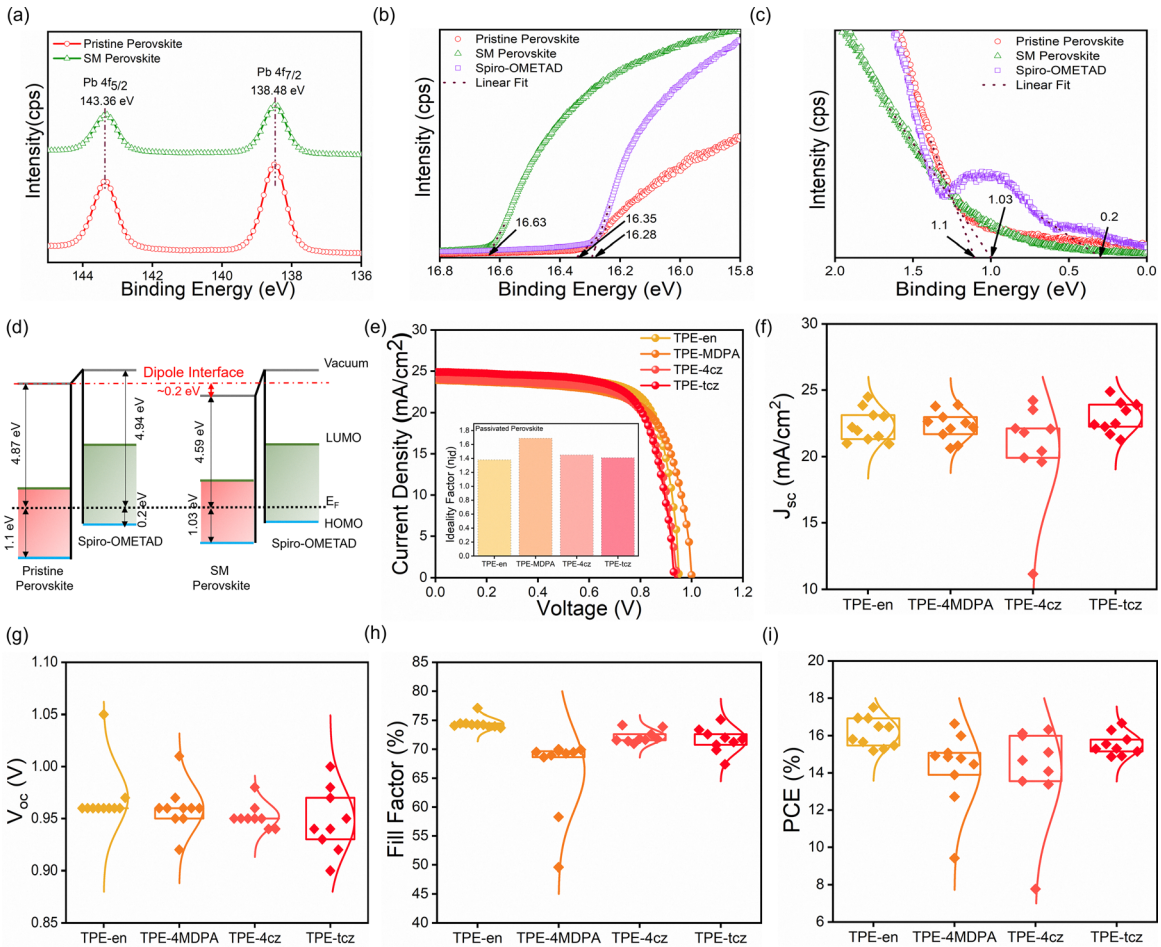

Fig. 4 (a) XPS spectra, (b) and (c) UPS spectra of pristine perovskite, SM perovskite, and Spiro-OMETAD, (d) Band alignment at the interface of perovskite (with and without surface modification) and Spiro-OMETAD (e) Light J–V characteristics and ideality factor of champion cell and (f) and (i) statistics of current density (J_{sc}), open-circuit voltage (V_{oc}), fill factor (FF), and power conversion efficiency (PCE) for SM perovskite with different TPE derivatives.

cell, and the photovoltaic performance is listed in Table 3. The device using SM perovskite using enamine derivative gave J_{sc} of 24.5 mA cm^{-2}, V_{oc} of 0.96 V, FF of 75%, and PCE of 17.5%. Whereas the devices using TPE-MDPA obtained J_{sc} of 23.8 mA cm^{-2}, V_{oc} of 0.97 V, FF of 69%, and PCE of 15.9%; TPE-4cz obtained J_{sc} of 24.2 mA cm^{-2}, V_{oc} of 0.95 V, FF of 71% and PCE of 16.32%; and TPE-tcz obtained J_{sc} of 24.8 mA cm^{-2}, V_{oc} of 0.94 V, FF of 71% and PCE of 16.7%. The ideality factor calculated from the dark J–V characteristic of the champion solar cell (Fig. 4e) for TPE-en is 31% less than TPE-MDPA, 7% less than TPE-4Cz, and 3% lesser than TPE-tcz. Leakage current is also less in the case of an enamine derivative-based device.

Table 3 Device parameters of the champion devices

TPE derivative used	J_{sc} (mA cm^{-2})	V_{oc} (V)	FF (%)	η (%)	n_{id}	J_o ($\times 10^{-9}$ A cm^{-2})
TPE-en	24.5	0.96	75	17.5	1.38	2.74 × 10^{-2}
TPE-MDPA	23.8	0.97	69	15.9	1.69	1.2
TPE-4cz	24.2	0.95	71	16.32	1.45	7.3 × 10^{-2}
TPE-tcz	24.8	0.94	71	16.7	1.41	9.49 × 10^{-3}

Although the differences are small, the histogram of 20 devices shows that the TPE-en derivative is the best. (Fig. 4(f–i)). The largest contributor to the improvement in P_{max} is the better FF, suggesting charge extraction is an important factor. We are trying to understand the chemistry, but one possible reason could be better band matching of TPE-en with perovskite and spiro-OMETAD. Another reason could be the comparatively smoother surface morphology of deposited TPE-en with better interfacial contact and charge transport.

In summary, we demonstrate an effective method to reduce the electronic defects at the perovskite surface and perovskite-Spiro interface by modifying the perovskite surface using a small organic molecule, *i.e.*, the enamine derivative of TPE. TPE-en minimizes the surface defects by the formation of a dipole interface which provide better band-alignment at the perovskite and HTL interface by pulling up the HOMO level of SM perovskite, which attenuates non-radiative carrier recombination and provides effective band alignment and improves hole extraction, resulting in the enhancement of the photovoltaic performance of PSCs. The SM perovskite-based PSC achieves an average power conversion efficiency (PCE) of 18.73% (with double cation perovskite). Devices with perovskite surfaces modified with TPE-en derivative obtained better device performance than other reported TPE derivatives.

Author contributions

Shubhangi Bhardwaj: conceptualization, data curation, formal analysis, investigation, methodology, visualization, writing – original draft, writing – review & editing, Praveen Naik: data curation, formal analysis, investigation, writing – review & editing, Anuj Kumar Palariya: data curation, formal analysis, investigation, writing – review & editing, Smrutiranjan Panda: data curation, formal analysis, writing – review & editing, Satish Patil: funding acquisition, project administration, resources, supervision, validation, writing – review & editing, Sushobhan Avasthi: funding acquisition, project administration, resources, supervision, validation, writing – review & editing.

Conflicts of interest

The authors declare that there is no conflict of interest regarding the publication of this manuscript.

Data availability

All the data supporting this article can be found within the article and the SI. And the origin files on this link **https://osf.io/k6ewx/?view_only=0b229e4e59f34dcfb292efd302b525f4**.

Experimental section, characterization tools details, field emission scanning electron microscopy images, X-ray diffraction patterns and data fitting and calculation details. See DOI: **https://doi.org/10.1039/d5qm00255a**.

Acknowledgements

The authors acknowledge the ANRF, Department of Science and Technology, Government of India, for the financial support under grant number CRG/2022/004523 and DST/ETC/CASE/RES/2023/02. The work was conducted at NNFC and MNCF with generous support from Ministry of Electronics and IT (MeitY), under the PRAMAN project, and Ministry of Education. SB acknowledges the technical support and input provided by Dr Laxman Gouda, Dr Chaya Karkera, Dr Pallavi Singh, Sanchari Debnath, Dr Ram Kumar CB, Kanad Majumder and Vithobha Hugar. PN acknowledges the UGC- Dr D. S. Kothari post-doctoral fellowship from the University Grant Commission, Government of India.

References

1 N.-G. Park, Perovskite Solar Cells: An Emerging Photovoltaic Technology, *Mater. Today*, 2015, **18**(2), 65–72, DOI: **10.1016/j.mattod.2014.07.007**.
2 H. S. Jung and N. Park, Perovskite Solar Cells: From Materials to Devices, *Small*, 2015, **11**(1), 10–25, DOI: **10.1002/smll.201402767**.
3 P. P. Boix, K. Nonomura, N. Mathews and S. G. Mhaisalkar, Current Progress and Future Perspectives for Organic/Inorganic Perovskite Solar Cells, *Mater. Today*, 2014, **17**(1), 16–23, DOI: **10.1016/j.mattod.2013.12.002**.
4 T. M. Brenner, D. A. Egger, L. Kronik, G. Hodes and D. Cahen, Hybrid Organic—Inorganic Perovskites: Low-Cost Semiconductors with Intriguing Charge-Transport Properties, *Nat. Rev. Mater.*, 2016, **1**(1), 15007, DOI: **10.1038/natrevmats.2015.7**.
5 D. Li, J. Shi, Y. Xu, Y. Luo, H. Wu and Q. Meng, Inorganic–Organic Halide Perovskites for New Photovoltaic Technology, *Natl. Sci. Rev.*, 2018, **5**(4), 559–576, DOI: **10.1093/nsr/nwx100**.
6 L. Jonathan, L. J. Diguna, O. Samy, M. Muqoyyanah, S. Abu Bakar, M. D. Birowosuto and A. El Moutaouakil, Hybrid Organic–Inorganic Perovskite Halide Materials for Photovoltaics towards Their Commercialization, *Polymers*, 2022, **14**(5), 1059, DOI: **10.3390/polym14051059**.
7 I. Hussain, H. P. Tran, J. Jaksik, J. Moore, N. Islam and M. J. Uddin, Functional materials, device architecture, and flexibility of perovskite solar cell, *Emergent Mater.*, 2018, **1**(3–4), 133–154, DOI: **10.1007/s42247-018-0013-1**.
8 P. Roy, N. Kumar Sinha, S. Tiwari and A. Khare, A Review on Perovskite Solar Cells: Evolution of Architecture, Fabrication Techniques, Commercialization Issues and Status, *Sol. Energy*, 2020, **198**, 665–688, DOI: **10.1016/j.solener.2020.01.080**.
9 D. Głowienka, D. Zhang, F. Di Giacomo, M. Najafi, S. Veenstra, J. Szmytkowski and Y. Galagan, Role of Surface Recombination in Perovskite Solar Cells at the Interface of HTL/CH3NH3PbI3, *Nano Energy*, 2020, **67**, 104186, DOI: **10.1016/j.nanoen.2019.104186**.
10 Z. Shariatinia, Recent Progress in Development of Diverse Kinds of Hole Transport Materials for the Perovskite Solar Cells: A Review, *Renewable Sustainable Energy Rev.*, 2020, **119**, 109608, DOI: **10.1016/j.rser.2019.109608**.

11 G. Ren, W. Han, Y. Deng, W. Wu, Z. Li, J. Guo, H. Bao, C. Liu and W. Guo, Strategies of Modifying Spiro-OMeTAD Materials for Perovskite Solar Cells: A Review, *J. Mater. Chem. A*, 2021, **9**(8), 4589–4625, DOI: **10.1039/D0TA11564A**.

12 L. Nakka, Y. Cheng, A. G. Aberle and F. Lin, Analytical Review of Spiro-OMeTAD Hole Transport Materials: Paths Toward Stable and Efficient Perovskite Solar Cells, *Adv. Energy Sustainable Res.*, 2022, **3**(8), 2200045, DOI: **10.1002/aesr.202200045**.

13 G. Niu, X. Guo and L. Wang, Review of Recent Progress in Chemical Stability of Perovskite Solar Cells, *J. Mater. Chem. A*, 2015, **3**(17), 8970–8980, DOI: **10.1039/C4TA04994B**.

14 F. M. Rombach, S. A. Haque and T. J. Macdonald, Lessons Learned from Spiro-OMeTAD and PTAA in Perovskite Solar Cells, *Energy Environ. Sci.*, 2021, **14**(10), 5161–5190, DOI: **10.1039/D1EE02095A**.

15 J. Chen and N. Park, Causes and Solutions of Recombination in Perovskite Solar Cells, *Adv. Mater.*, 2019, **31**(47), 1803019, DOI: **10.1002/adma.201803019**.

16 C. M. Wolff, P. Caprioglio, M. Stolterfoht and D. Neher, Nonradiative Recombination in Perovskite Solar Cells: The Role of Interfaces, *Adv. Mater.*, 2019, **31**(52), 1902762, DOI: **10.1002/adma.201902762**.

17 G. O. Odunmbaku, S. Chen, B. Guo, Y. Zhou, N. A. N. Ouedraogo, Y. Zheng, J. Li, M. Li and K. Sun, Recombination Pathways in Perovskite Solar Cells, *Adv. Mater. Interfaces*, 2022, **9**(12), 2102137, DOI: **10.1002/admi.202102137**.

18 F. Gao, Y. Zhao, X. Zhang and J. You, Recent Progresses on Defect Passivation toward Efficient Perovskite Solar Cells, *Adv. Energy Mater.*, 2020, **10**(13), 1902650, DOI: **10.1002/aenm.201902650**.

19 S. Akin, N. Arora, S. M. Zakeeruddin, M. Grätzel, R. H. Friend and M. I. Dar, New Strategies for Defect Passivation in High-Efficiency Perovskite Solar Cells, *Adv. Energy Mater.*, 2020, **10**(13), 1903090, DOI: **10.1002/aenm.201903090**.

20 Z. Zhang, L. Qiao, K. Meng, R. Long, G. Chen and P. Gao, Rationalization of Passivation Strategies toward High-Performance Perovskite Solar Cells, *Chem. Soc. Rev.*, 2023, **52**(1), 163–195, DOI: **10.1039/D2CS00217E**.

21 H. Kim, C. A. Figueroa Morales, S. Seong, Z. Hu, N. Muyanja, S. Penukula, T. Zheng, Z. Pizzo, C. S. Yim, A. Lenert, N. Rolston and X. Gong, Molecular Design of Defect Passivators for Thermally Stable Metal-Halide Perovskite Films, *Matter*, 2024, **7**(2), 539–549, DOI: **10.1016/j.matt.2023.12.003**.

22 L. Su, Y. Xiao, L. Lu, G. Han and M. Zhu, Enhanced Stability and Solar Cell Performance via π-Conjugated Lewis Base Passivation of Organic Inorganic Lead Halide Perovskites, *Org. Electron.*, 2020, **77**, 105519, DOI: **10.1016/j.orgel.2019.105519**.

23 G. Yang, P. Qin, G. Fang and G. Li, A Lewis Base-Assisted Passivation Strategy Towards Highly Efficient and Stable Perovskite Solar Cells, *Sol. RRL*, 2018, **2**, 1800055, DOI: **10.1002/SOLR.201800055**.

24 Y. Lin, L. Shen, J. Dai, Y. Deng, Y. Wu, Y. Bai, X. Zheng, J. Wang, Y. Fang, H. Wei, W. Ma, X. C. Zeng, X. Zhan and J. Huang, π-Conjugated Lewis Base: Efficient Trap-Passivation and Charge-Extraction for Hybrid Perovskite Solar Cell, *Adv. Mater.*, 2017, **29**, 1604545, DOI: **10.1002/ADMA.201604545**.

25 Z. Li, B. Li, X. Wu, S. A. Sheppard, S. Zhang, D. Gao, N. J. Long and Z. Zhu, Organometallic-Functionalized Interfaces for Highly Efficient Inverted Perovskite Solar Cells, *Science*, 2022, **376**(6591), 416–420, DOI: **10.1126/science.abm8566**.

26 X. Zheng, B. Chen, J. Dai, Y. Fang, Y. Bai, Y. Lin, H. Wei, X. C. Zeng and J. Huang, Defect Passivation in Hybrid Perovskite Solar Cells Using Quaternary Ammonium Halide Anions and Cations, *Nat. Energy*, 2017, **2**, 17102, DOI: **10.1038/nenergy.2017.102**.

27 X. Zhang, X. Liu, R. Ghadari, M. Li, Z. Zhou, Y. Ding, M. Cai and S. Dai, Tetraphenylethylene-Arylamine Derivatives as Hole Transporting Materials for Perovskite Solar Cells, *ACS Appl. Mater. Interfaces*, 2021, **13**(10), 12322–12330, DOI: **10.1021/acsami.1c01606**.

28 R. Ali and R. Siddiqui, Dithieno[3,2-*b*:2′,3′-*d*]Thiophene (DTT): An Emerging Heterocyclic Building Block for Future Organic Electronic Materials & Functional Supramolecular Chemistry, *RSC Adv.*, 2022, **12**(55), 36073–36102, DOI: **10.1039/D2RA05768A**.

29 K. Jiang, J. Wang, F. Wu, Q. Xue, Q. Yao, J. Zhang, Y. Chen, G. Zhang, Z. Zhu, H. Yan, L. Zhu and H.-L. Yip, Dopant-Free Organic Hole-Transporting Material for Efficient and Stable Inverted All-Inorganic and Hybrid Perovskite Solar Cells, *Adv. Mater.*, 2020, **32**, 1908011, DOI: **10.1002/adma.201908011**.

30 N. K. Noel, A. Abate, S. D. Stranks, E. S. Parrott, V. M. Burlakov, A. Goriely and H. J. Snaith, Enhanced Photoluminescence and Solar Cell Performance via Lewis Base Passivation of Organic–Inorganic Lead Halide Perovskites, *ACS Nano*, 2014, **8**(10), 9815–9821, DOI: **10.1021/nn5036476**.

31 J. Tauc, Optical Properties and Electronic Structure of Amorphous Ge and Si, *Mater. Res. Bull.*, 1968, **3**(1), 37–46, DOI: **10.1016/0025-5408(68)90023-8**.

32 D. L. Wood and J. Tauc, Weak Absorption Tails in Amorphous Semiconductors, *Phys. Rev. B: Condens. Matter Mater. Phys.*, 1972, **5**(8), 3144–3151, DOI: **10.1103/PhysRevB.5.3144**.

33 N. Gu, Z. Sun, L. Song, P. Du and J. Xiong, Aggregation-induced Emission Materials for High-efficiency Perovskite Solar Cells, *Chem. Phys. Chem.*, 2023, **24**(14), e202200919, DOI: **10.1002/cphc.202200919**.

34 Z. Ma, D. Huang, Q. Liu, G. Yan, Z. Xiao, D. Chen, J. Zhao, Y. Xiang, C. Peng, H. Li, M. Zhang, W. Zhang, L. Duan and Y. Huang, Excess PbI2 Evolution for Triple-Cation Based Perovskite Solar Cells with 21.9% Efficiency, *J. Energy Chem.*, 2022, **66**, 152–160, DOI: **10.1016/j.jechem.2021.07.030**.

35 F. Urbach, The Long-Wavelength Edge of Photographic Sensitivity and of the Electronic Absorption of Solids, *Phys. Rev.*, 1953, **92**, 1324, DOI: **10.1103/PhysRev.92.1324**.

36 S. John, C. Soukoulis, M. H. Cohen and E. N. Economou, Theory of Electron Band Tails and the Urbach Optical-

Absorption Edge, *Phys. Rev. Lett.*, 1986, **57**(14), 1777–1780, DOI: 10.1103/PhysRevLett.57.1777.

37 I. Bonalde, E. Medina, M. Rodríguez, S. M. Wasim, G. Marín, C. Rincón, A. Rincón and C. Torres, Urbach Tail, Disorder, and Localized Modes in Ternary Semiconductors, *Phys. Rev. B: Condens. Matter Mater. Phys.*, 2004, **69**(19), 195201, DOI: 10.1103/PhysRevB.69.195201.

38 E. Aydin, M. Bastiani and S. Wolf, Defect and Contact Passivation for Perovskite Solar Cells, *Adv. Mater.*, 2019, **31**(25), 1900428, DOI: 10.1002/adma.201900428.

39 Y. Li, Z. Li, F. Liu and J. Wei, Defects and Passivation in Perovskite Solar Cells, *Surf. Innov.*, 2022, **10**(1), 3–20, DOI: 10.1680/jsuin.21.00058.

40 H. Zhang, Y. Wu, C. Shen, E. Li, C. Yan, W. Zhang, H. Tian, L. Han and W. Zhu, Efficient and Stable Chemical Passivation on Perovskite Surface via Bidentate Anchoring, *Adv. Energy Mater.*, 2019, **9**(13), 1803573, DOI: 10.1002/aenm.201803573.

41 S. You, H. Wang, S. Bi, J. Zhou, L. Qin, X. Qiu, Z. Zhao, Y. Xu, Y. Zhang, X. Shi, H. Zhou and Z. Tang, A Biopolymer Heparin Sodium Interlayer Anchoring TiO_2 and $MAPbI_3$ Enhances Trap Passivation and Device Stability in Perovskite Solar Cells, *Adv. Mater.*, 2018, **30**(22), 1706924, DOI: 10.1002/adma.201706924.

42 J. Blochwitz, T. Fritz, M. Pfeiffer, K. Leo, D. M. Alloway, P. A. Lee and N. R. Armstrong, Interface Electronic Structure of Organic Semiconductors with Controlled Doping Levels, *Org. Electron.*, 2001, **2**(2), 97–104, DOI: 10.1016/S1566-1199(01)00016-7.

43 P. Zhao, B. J. Kim and H. S. Jung, Passivation in Perovskite Solar Cells: A Review, *Mater. Today Energy*, 2018, **7**, 267–286, DOI: 10.1016/j.mtener.2018.01.004.

44 P. Schulz, D. Cahen and A. Kahn, Halide Perovskites: Is It All about the Interfaces, *Chem. Rev.*, 2019, **119**(5), 3349–3417, DOI: 10.1021/acs.chemrev.8b00558.

45 D. Cahen and A. Kahn, Electron Energetics at Surfaces and Interfaces: Concepts and Experiments, *Adv. Mater.*, 2003, **15**(4), 271–277, DOI: 10.1002/adma.200390065.

46 P. Schulz, E. Edri, S. Kirmayer, G. Hodes, D. Cahen and A. Kahn, Interface Energetics in Organo-Metal Halide Perovskite-Based Photovoltaic Cells, *Energy Environ. Sci.*, 2014, **7**(4), 1377, DOI: 10.1039/c4ee00168k.

47 J. Shi, X. Xu, D. Li and Q. Meng, Interfaces in Perovskite Solar Cells, *Small*, 2015, **11**(21), 2472–2486, DOI: 10.1002/smll.201403534.

48 Q. Chen, C. Wang, Y. Li and L. Chen, Interfacial Dipole in Organic and Perovskite Solar Cells, *J. Am. Chem. Soc.*, 2020, **142**(43), 18281–18292, DOI: 10.1021/jacs.0c07439.

49 J. Morais, J. Ma and M. B. Zimmt, Solvent Dependence of the Twisted Excited State Energy of Tetraphenylethylene: Evidence for a Zwitterionic State from Picosecond Optical Calorimetry, *J. Phys. Chem.*, 1991, **95**(10), 3885–3888, DOI: 10.1021/j100163a001.

50 W. Schuddeboom, S. A. Jonker, J. M. Warman, M. P. De Haas, M. J. W. Vermeulen, W. F. Jager, B. De Lange, B. L. Feringa and R. W. Fessenden, Sudden Polarization in the Twisted, Phantom State of Tetraphenylethylene Detected by Time-Resolved Microwave Conductivity, *J. Am. Chem. Soc.*, 1993, **115**(8), 3286–3290, DOI: 10.1021/ja00061a029.

51 J. Huang, X. Yang, J. Wang, C. Zhong, L. Wang, J. Qin and Z. Li, New Tetraphenylethene-Based Efficient Blue Luminophors: Aggregation Induced Emission and Partially Controllable Emitting Color, *J. Mater. Chem.*, 2012, **22**(6), 2478–2484, DOI: 10.1039/C1JM14054J.

52 S. Odabas, E. Tekin, F. Turksoy and C. Tanyeli, Inexpensive and Valuable: A Series of New Luminogenic Molecules with the Tetraphenylethene Core Having Excellent Aggregation Induced Emission Properties, *J. Mater. Chem. C*, 2013, **1**(42), 7081, DOI: 10.1039/c3tc31427h.

53 Q. Chen, D.-P. Liu, M. Luo, L.-J. Feng, Y.-C. Zhao and B.-H. Han, Nitrogen-Containing Microporous Conjugated Polymers via Carbazole-Based Oxidative Coupling Polymerization: Preparation, Porosity, and Gas Uptake, *Small*, 2014, **10**(2), 308–315, DOI: 10.1002/smll.201301618.

54 H. Choi, K. Do, S. Park, J. Yu and J. Ko, Efficient Hole Transporting Materials with Two or Four *N*,*N*-Di(4-methoxyphenyl)Aminophenyl Arms on an Ethene Unit for Perovskite Solar Cells, *Chem. – Eur. J.*, 2015, **21**(45), 15919–15923, DOI: 10.1002/chem.201502741.

55 Y. Qi, Y. Wang, Y. Yu, Z. Liu, Y. Zhang, Y. Qi and C. Zhou, Exploring Highly Efficient Light Conversion Agents for Agricultural Film Based on Aggregation Induced Emission Effects, *J. Mater. Chem. C*, 2016, **4**(47), 11291–11297, DOI: 10.1039/C6TC04215E.

56 F. Wu, J. Liu, G. Wang, Q. Song and L. Zhu, M-Methoxy Substituents in a Tetraphenylethylene-Based Hole-Transport Material for Efficient Perovskite Solar Cells, *Chem. – Eur. J.*, 2016, **22**(46), 16636–16641, DOI: 10.1002/chem.201603672.

57 X. Zhang, Z. Zhou, S. Ma, G. Wu, X. Liu, M. Mateen, R. Ghadari, Y. Wu, Y. Ding, M. Cai and S. Dai, Fused Tetraphenylethylene–Triphenylamine as an Efficient Hole Transporting Material in Perovskite Solar Cells, *Chem. Commun.*, 2020, **56**(21), 3159–3162, DOI: 10.1039/C9CC09901H.

